

## Plasmonic Nanopores for Single-Molecule Detection and Manipulation: Toward Sequencing Applications

Denis Garoli,<sup>\*,†</sup> Hirohito Yamazaki,<sup>‡</sup> Nicolò Maccaferri,<sup>§</sup> and Meni Wanunu<sup>\*,‡,§</sup>

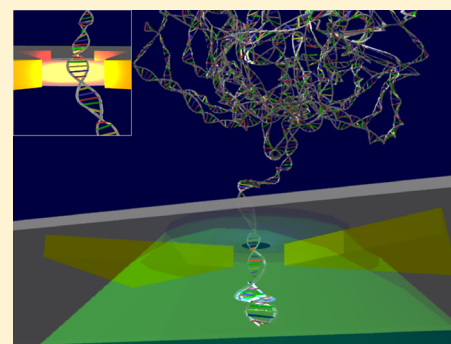
<sup>†</sup>Istituto Italiano di Tecnologia, via Morego 30, I-16163, Genova, Italy

<sup>‡</sup>Department of Physics, Northeastern University, 360 Huntington Avenue, Boston, Massachusetts 02115, United States

<sup>§</sup>Physics and Materials Science Research Unit, University of Luxembourg, 162a avenue de la Faïencerie, L-1511 Luxembourg, Luxembourg

**ABSTRACT:** Solid-state nanopore-based sensors are promising platforms for next-generation sequencing technologies, featuring label-free single-molecule sensitivity, rapid detection, and low-cost manufacturing. In recent years, solid-state nanopores have been explored due to their miscellaneous fabrication methods and their use in a wide range of sensing applications. Here, we highlight a novel family of solid-state nanopores which have recently appeared, namely plasmonic nanopores. The use of plasmonic nanopores to engineer electromagnetic fields around a nanopore sensor allows for enhanced optical spectroscopies, local control over temperature, thermophoresis of molecules and ions to/from the sensor, and trapping of entities. This Mini Review offers a comprehensive understanding of the current state-of-the-art plasmonic nanopores for single-molecule detection and biomolecular sequencing applications and discusses the latest advances and future perspectives on plasmonic nanopore-based technologies.

**KEYWORDS:** Plasmonics, nanopore, solid-state, sequencing, single-molecule



Surface plasmon resonance (SPR) refers to the collective oscillations of the conduction electrons in metallic nanostructures.<sup>1</sup> Both the intensity and the energy of the SPR phenomenon strongly depend on the size, shape, and composition of the nanostructures, as well as on the dielectric properties of the surrounding environment. Various factors affect the plasmonic nanostructure response, which allow for a rationally guided design of plasmonic sensors with tunable sensitivity. These nanoscale detectors have found applications in several fields such as light harvesting, photocatalysis, subwavelength imaging, metamaterials, and nanomedicine.<sup>2</sup> Among others, one specific family of plasmonic platforms is based on plasmonic nanohole arrays and the more recently implemented plasmonic nanopores, sub-100 nm apertures connecting two compartments, for sensing applications. Although the reader can find exhaustive details on the principles, fabrication, and applications of plasmonic nanoholes and nanopores for biosensing in recent reviews by Dahlin<sup>3</sup> and by Spitzberg and co-workers,<sup>4</sup> here we focus our attention on the potential applications and integration of plasmonic nanopores as transducers in single-molecule detection, manipulation, and sequencing.

During the last few decades a new generation of single-molecule information reader technologies have emerged, the most advanced example being single-molecule sequencing (SMS).<sup>5</sup> SMS involves threading single nucleic acid strands through elements (reader molecules, enzymes, nanopores, and other nanostructures) that can be used for detecting specific

signals (e.g., electrical, optical, or mechanical). Individual base pairs, the monomer units of DNA/RNA polymers, are then detected sequentially one at a time as they interact with these elements. In particular, in the past several years SMS platforms, such as those by Pacific Biosciences and Oxford Nanopore Technologies, have become available to researchers and are currently being utilized in research and clinical settings. SMS nanotechnologies can be divided into two main categories: (i) Sequencing-by-synthesis in which a DNA polymerase replicates a DNA molecule and the added sequence is read out, either in real time<sup>6</sup> or by sequential addition of bases,<sup>7</sup> and (ii) nanopore-sequencing technologies in which single molecules of DNA (or RNA) are threaded through a nanopore or positioned in the vicinity of a nanopore, and  $k$ -mers of DNA bases ( $k = 4-5$ ) are detected as they are translocated through the pore in single base steps.<sup>8,9</sup> However, nucleic acid sequencing goes beyond the four DNA/RNA bases, as various chemical modifications and damaged DNA sites produce additional signals that require orthogonal readout modes for correct modified base assignment. Therefore, at the core of nanopore sequencing technologies lies a challenge of producing solid-state nanopores with a quality that rivals their much more reliable biological pore counterparts. In particular, ion channels and bacterial toxin channels, for

**Received:** July 6, 2019

**Revised:** September 16, 2019

**Published:** October 6, 2019

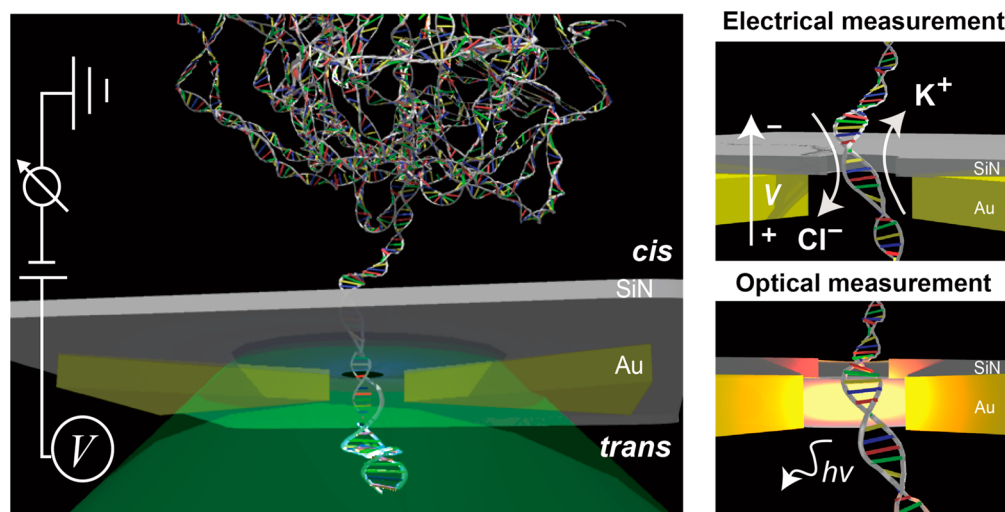


**Figure 1.** Plasmonic nanopore-based electrical and optical measurement. (Left) DNA translocation through a plasmonic nanopore. Coiled double-stranded DNA that enters the pore from the *cis* chamber passes through the pore equipped with a plasmonic nanostructure comprising two gold triangle plates. The visible laser (green) is illuminated on bottom side of plasmonic nanopore so that a strong electromagnetic field is generated at the exit of the pore. (Top right) Principle of electrical measurement. When voltage is applied across the plasmonic nanopore, DNA and ions ( $K^+$  and  $Cl^-$ ) are driven through the pore, producing a strong, pore-localized electric field. (Bottom right) An illustration of a plasmonic-enhanced optical measurement. DNA traversing the hotspot between two gold nanostructures leads to emission of enhanced optical signals containing information about the molecule (for example, FE, Raman scattering and light scattering).

example,  $\alpha$ -hemolysin,<sup>10</sup> MspA,<sup>9</sup> and CsgG,<sup>11</sup> when embedded in a lipid bilayer membrane, serve as nanopore sensors with outstanding signal reproducibility and good sensitivity. Some engineered (i.e., mutated amino-acid sequence) versions of these channels have the right performance that allows SMS with reasonable single-pass accuracy, although typically more than a single-pass read is required to ascertain DNA sequence in a given sample. In contrast, SMS using solid-state nanopores has yet to be shown, despite the exciting recent developments of new methods for producing small and thin nanopores in solid-state materials.<sup>12–15</sup> The potential for tuning the physical and chemical properties of solid-state pores, as well as their compatibility with mass-production, shows significant potential advantages. Moreover, one of the main motivations for a new class of nanopore sensors is to overcome the limitations of the current electrical readout:

(i) The time resolution of nanopore sensors depends on the maximum bandwidth of the measurements, which in turn is an optimized parameter that depends on the ion flux and membrane capacitance. For standard sequencing using protein nanopores, this maximum bandwidth of  $\sim 5$  kHz presents a maximum sequencing rate of  $\sim 1000$  bases per second assuming 5 data points per read, insufficient for high-accuracy basecalling.

(ii) Low throughput: simultaneous multiplexed readout from many thousands of nanopores without compromising the temporal bandwidth and current sensitivity is currently a challenge in electrical current readout approaches, which prevents the development of low-cost and high-throughput devices.

(iii) Even the shortest nanopore channel, a single-atom thick pore, is insufficient for spatially resolving a single base due to access resistance limitations. Thus, the development of complementary strategies to further improve the nanopore spatial resolution is required.

Several strategies have been proposed to address these limitations. In this Mini Review, we argue that it would be

advantageous to complement nanopore sensing with new measuring modalities (e.g., optical detection) beyond electrical recordings. In this regard, as stated by Spitzberg et al.,<sup>4</sup> plasmonic nanopores offer improvements not only in sensitivity but also in specificity, observation rate, dwell time, and scalable parallelized detection. Some pioneer works have already demonstrated the potential of integrated readout solutions, although a platform capable of competing with commercially available techniques is still far from being realized.<sup>16–18</sup> Plasmonic-based solid-state nanopore sensors present new opportunities for biomolecular sensing. In fact, a plasmonic nanostructure can enhance and focus electromagnetic (e.m.) radiation to a nanoscale volume (hotspot) localized at the nanopore, in which biomolecules can be “scanned” as they translocate through the pore (Figure 1). This approach is very powerful for the following reasons: (i) the measurement is independent from electrical sensing and relies on detection of photons rather than electrons; (ii) the optical detection can be performed in the far-field, as photons freely travel in the aqueous media surrounding the nanopores. These unique features opens up vast opportunities for light excitation and broad spectral emission that cause minimal interference with the local electrical measurement that can be performed at the nanopore itself.<sup>19</sup> Moreover, single molecule sensing via optical readout is extremely challenging due to the low signal-to-noise ratio (S/N) in regular (nonplasmonic) nanopore platforms. A plasmonic nanopore represents an intriguing tool for increasing the S/N via the e.m. field enhancement that can be generated by engineered nanostructures. In particular, plasmonic integration offers a new way to face one of the main limitations of solid-state nanopores, that is, the far-too-rapid and not well-controlled translocation mechanism of DNA and proteins molecules through them. Although a large effort is still needed in order to solve this issue, the new functionalities offered by plasmonics, such as trapping and thermophoresis,<sup>20</sup> have shown great potential and

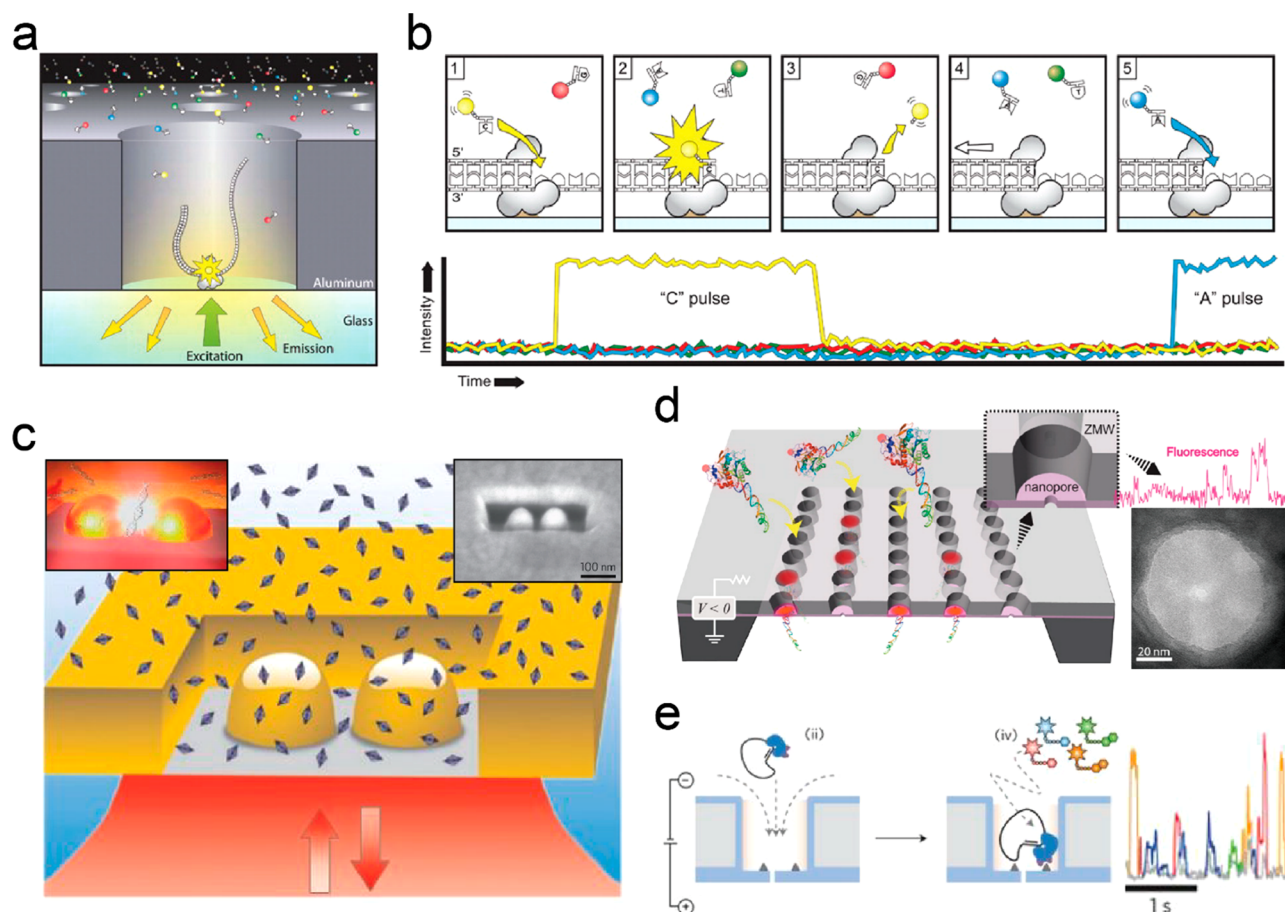


**Figure 2.** Single-molecule enhanced detection using zero-mode waveguides (ZMWs). (a) Schematic of Pacific Biosciences' long-read sequencing using ZMWs, where a DNA polymerase resides at the base of a glass substrate that is decorated with 100 nm wells formed in a silica-supported Al film. Light from the bottom side is exclusively attenuated, and the confined electromagnetic field (evanescent field) allows single fluorophore detection at high fluorophore concentrations ( $>100$  nM). (b) Nucleotide incorporation is observed by fluorescence from a single phospholinked labeled nucleotide. Because nucleotide incorporation requires some waiting time (1–10 ms), a dye molecule resides on the ZMW bottom during polymerase-mediated incorporation long enough to produce a photon burst, before being cleaved from the incorporated nucleotide and diffusing away to the bulk. Adapted with permission from ref 6, copyright 2009, American Association for the Advancement of Science. (c) Plasmonic antenna in box platform. Gold dimer nanoparticle-antenna where two semisphere nanoparticles are facing in a gold rectangular box allows the lowering of a background signal as well as enhancing a fluorescence signal. Adapted with permission from refs 30 and 31, copyright 2013 Springer Nature and Wiley Periodicals, Inc. (d,e) NZMW for single molecule manipulation and DNA sequencing. A pore formed in an Al nanometric hole on a freestanding membrane captures and releases single molecules via electrophoretic forces. This platform enhances the loading efficiency by orders of magnitude, and also allows the loading of long DNA ( $>10$  kb). Adapted with permission from refs 33 and 34, copyright 2014 American Chemical Society and 2017 Springer Nature.

new methods in this field can significantly impact the potential of commercial use of these technologies.

The aim of this Mini Review is to highlight the enhanced performance of plasmonic nanopore sensors, as well as mention the use of new materials for plasmonic sensors. We highlight recent experiments on single-molecule detection in plasmonic platforms where engineered e.m. fields not only boost the sensitivity but also generate thermomechanical-related effects for translocation control in nanopores. Furthermore, we will show how plasmonic nanocavities and nanoantennas combined with nanopores can have unique advantages over solid-state nanopores alone. Finally, we will propose how plasmonic nanopores can be integrated with additional elements, such as biological pores or two-dimensional (2D) materials, in order to prepare hybrid and integrated sensors with truly unique capabilities.

**Plasmonics for Single Molecule Enhanced Optical Detection: From Zero-Mode Waveguides to Nanopores.**

Among the technologies based on solid-state platforms, the most successful SMS platform is the Pacific Biosciences' for single molecule, real-time (SMRT) sequencing.<sup>6</sup> This technology is based on the observation of fluorescence emission (FE) of single molecules of DNA polymerase activity as they synthesize a single molecule of DNA inside a zero-mode waveguide (ZMW) (Figure 2a,b).<sup>21</sup> A ZMW consists of a nanometric well usually fabricated by forming a hole in a thin Al film. The key design principle of a ZMW is a confined e.m. field at the bottom of the nanowell. Given a certain illumination, the only molecules that are affected by the light field are the ones located at the bottom of the nanohole. The reservoir of fluorescent molecules above the membrane is screened by the metallic film. As a result, only fluorophores that reside at the bottom of the well produce a detectable signal. A ZMW reduces the detection volume by 3 to 6 orders of magnitude from  $10^{-15}$  (with a standard confocal microscope) to between  $10^{-18}$  and  $10^{-21}$  L, allowing single-molecule

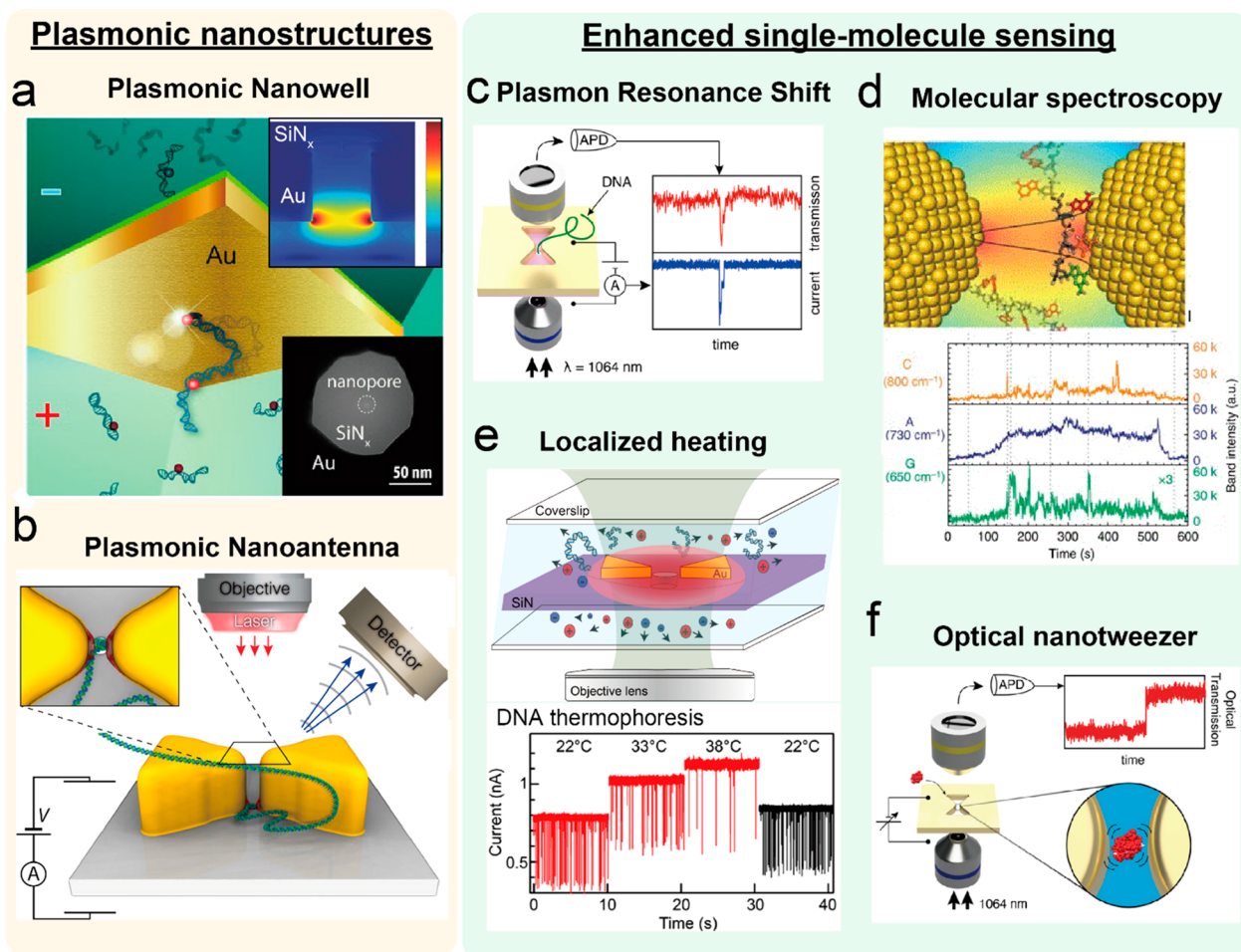


**Figure 3.** Plasmonic nanopore enhancing detection capabilities. (a,b) Plasmonic nanostructures. (a) Plasmonic nanowell—nanopore. One hundred nanometer aperture gold nanowell on silicon nitride membrane with a 4 nm pore does not suppress the background signal and instead increases fluorescence signals up to 10-fold. Adapted with permission from ref 37, copyright WILEY-VCH Verlag GmbH & Co. KGaA, Weinheim. (b) Plasmonic bowtie antenna—nanopore. Electromagnetic field at bowtie antenna structure with narrow gap (about a few nanometers) controls DNA translocation velocity, enhances optical signal of DNA and fabricates self-aligned nanopores. Adapted with permission from ref 40, copyright 2015 American Chemical Society. (c–f) Enhanced single-molecule sensing. (c) Label-free detection using a plasmon resonance shift. Optical trace during DNA translocation through a pore can be seen because the plasmonic resonance shift causes the reduction of transmission light at the initial peak wavelength. The optical signal produced by the platform independent on buffer conditions, allowing one to probe properties of the biological molecule at physiological conditions. Adapted with permission from ref 42, copyright 2018 American Chemical Society. (d) Plasmonic nanoslit for DNA SERS. Sub-10 nm gold nanoslit generate SERS of ssDNA (5'-poly(dA)48dCdG-3') which is captured by electrophoresis and temporarily absorbed at the plasmonic interface. Adapted with permission from ref 36, copyright 2018 Springer Nature. (e) Laser-induced local heating. A pore having photothermal effect heats up the surrounding environment when the laser power is strong enough, resulting in a huge temperature gradient at a pore. This gradient causes molecule/ion thermophoresis, as seen by capturing rate/current kinetics. Adapted with permission from ref 50 copyright 2017 American Chemical Society. (f) Nano-optical tweezing platform. A single protein molecule is navigated into a pore by the electric field and trapped at a strong electromagnetic field of a tapered structure, resulting in the increase of a transmission optical signal. Nanopore implementation into plasmonic structure assists capturing a protein at the hotspot with high efficiency. The platform is useful to study protein conformational dynamics. Adapted with permission from ref 57, copyright WILEY-VCH Verlag GmbH & Co. KGaA, Weinheim.

detection in zeptoliter volumes. Although they have had important commercial success, standard ZMWs prepared in Al thin film can still be significantly improved. In addition to confinement, enhanced e.m. fields, such as those achieved using plasmonic nanostructures, can play a crucial role in increasing the brightness of fluorophores by affecting their radiative rate. Unfortunately, standard Al ZMWs<sup>21</sup> are not optimized with this characteristic in mind, although Al is a well-known plasmonic material, as an Al nanowell enables very low e.m. field enhancement in the visible range. On the contrary, optimized plasmonic nanocavities resembling the ZMWs' principle of different shapes have been designed for single-molecule studies, and ZMWs fabricated with the use of

noble metals (Ag or Au) films provide both a stronger e.m. field and FE. It is worth mentioning that plasmonic enhanced e.m. fields can interact with fluorophores at their absorption  $\lambda_{ab}$  and emission  $\lambda_{em}$  wavelengths altering respective transitions between the ground state and higher excited states. The reader can find a detailed discussion on plasmon-enhanced fluorescence physics in a review by Bauch et al.<sup>22</sup> As stated by Bauch et al., the enhancement in FE depends on three main effects: (i) the increased excitation rate  $\gamma_e$  through the plasmon-enhanced field intensity ( $|E|^2$ ) at the absorption wavelength of  $\lambda_{abs}$ , (ii) the enhancement of fluorophore quantum yield  $\eta$ , and (iii) directionality  $\vec{f}$  of plasmon-coupled emission at the wavelength  $\lambda_{em}$ . Consequently, the FE of

detected fluorescence intensity with respect to that measured without the metallic structures (e.g., a free fluorophore in homogeneous aqueous environment,  $\gamma_0$  and  $\eta_0$ ) can be written as  $FE = \gamma_e/\gamma_0 \times \eta/\eta_0 \times f$ .<sup>22</sup> Tuning these terms allows to one efficiently engineer a single-molecule sensor in order to improve both the sensitivity and the signal-to-noise ratio. In particular, regarding plasmonic ZMWs, FE close to 30-fold with respect to a standard Al ZMW has been recently reported by optimizing the max e.m. field enhancement at the bottom of the nanowell using a bimetallic Au/Al film structure.<sup>23</sup> Furthermore, it is experimentally proven that the sophisticated plasmonic nanoantennas can achieve over 1000-fold FE.<sup>24,25</sup> In particular, during the past few years Wenger and colleagues reported pioneering designs where plasmonic antennas (Figure 2c) can enable FE factors in the range of  $10^4$ – $10^5$ -fold together with detection volumes down to few tens of zeptoliters.<sup>26</sup> Similar designs have been also used to increase the efficiency of nanoscale energy transfer between molecules. It is well-known that when the distance between an excited donor molecule (D) to the ground-state acceptor molecule (A) is in the range of 2–20 nm, energy transfer is described by Förster resonance energy-transfer (FRET) formalism, which accounts for a near-field nonradiative dipole–dipole interaction. FRET is an extremely interesting phenomena for SMS and it has also been used in a first experimental demonstration of single-molecule protein sequencing.<sup>27</sup> The FRET efficiency is the quantum yield (the number of times a specific event occurs per photon absorbed by the system) of the energy-transfer transition, that is, the probability of energy-transfer event occurring per donor excitation event<sup>28,29</sup>

$$E_{\text{FRET}} = \frac{k_{\text{ET}}}{k_f + k_{\text{ET}} + \sum k_i}$$

where  $k_{\text{ET}}$  is the rate of energy transfer,  $k_f$  is the radiative decay rate of the donor, and  $k_i$  are the rates of any other de-excitation pathways excluding energy transfers to other acceptors. Beyond the distance between the donor and the acceptor, the FRET efficiency depends on many factors, such as (i) the overlap between the donor emission and the acceptor absorption spectra, and (ii) the relative orientation of the donor–acceptor dipole momenta. In this framework, plasmonics can play an additional role in enhancing the FRET by increasing the decay rate of D, A, or both. In order to achieve this, nanostructures with enhanced e.m. fields in broadband spectral range have been proposed, achieving FRET efficiency enhancement close to 1 order of magnitude.<sup>30,31</sup> Moreover, it has been recently demonstrated that  $E_{\text{FRET}}$  can be enhanced by a factor of 3 in optimized Al ZMW extending the FRET range beyond 10 nm.<sup>32</sup> These discoveries have opened new pathways to engineer this phenomena at single-molecule levels.<sup>30,31</sup>

A plasmonic ZMW can be prepared on a transparent substrate by means of different lithographic methods. Interestingly, if the typically used glass substrate is replaced by a thin membrane (made for example of  $\text{SiO}_2$ ,  $\text{TiO}_2$ , or  $\text{Si}_3\text{N}_4$ ), the ZMW can be integrated with a nanopore, thus realizing a nanopore ZMW (NZMW). This nanopore integration delivers single molecule manipulation to the ZMW platform. By applying voltage, the electric field across the metallic nanowells equipped with nanopores at their bases draws molecules into them through electrokinetic mechanisms, leading to reversible and rapid molecular loading (Figure 2d).<sup>33</sup> This NZMW platform, where the molecular pulling

force enables length-independent DNA loading with low concentration (about a few picomolar), is advantageous for SMRT sequencing because typical diffusion-based DNA loading is strongly restricted by size difference between the DNA coil ( $\sim 560$  nm for  $\sim 10$  kbp DNA fragment) and the 100–150 nm ZMW cavity (Figure 2e).<sup>34</sup> Because fabrication of  $\sim 10$  nm pore in nanometric holes precisely is a critical issue, the implementation of nanoporous membranes as the ZMW base allows a highly parallel approach to mass produce at the wafer scale chips that contain active ZMW arrays and can represent the simplest design for a plasmonic nanopore platform.<sup>35</sup>

**Plasmonic Nanopores: Simultaneous Electro-optical Molecular Entity Readout.** While many studies on plasmon-based biomolecular binding events sensing have been reported so far, only recently plasmonic nanopores have been used as powerful single-molecule biosensors.<sup>3,4</sup> Different optical spectroscopic techniques have been implemented in plasmonic nanopores. In particular, as mentioned above, highly confined plasmonic fields can be used to enhance FE and FRET from biomolecules tagged with suitable fluorescent dyes. Moreover, in the case of nonfluorescent molecules to be detected during nanopore translocation, surface enhanced raman spectroscopy (SERS) has demonstrated the ability to enable single-molecule sensitivity by probing the Raman signals of four nucleotides and DNA oligonucleotides.<sup>36</sup>

Another version of a NZMW, this time made from Au rather than Al, is referred by Assad et al. as a “plasmonic nanowell”.<sup>37</sup> This design confines the e.m. field similarly to a standard ZMW with a consequent strong suppression of background fluorescence from the bulk and a net greater than 10-fold enhancement of the FE (Figure 3a). The device, a prime example of combined electro-optical measurements, offers extremely high signal-to-background ratio for single-molecule detection at ultralow excitation laser intensities ( $\sim 10^8$   $\mu\text{W}/\text{cm}^2$ ), while maintaining an extremely high temporal bandwidth ( $\sim 10$   $\mu\text{s}$  time-resolution) for single-DNA sensing. This design relieves the requirement of typical plasmonic nanopore concept that plasmonic structures lie next to a pore within  $\sim 10$  nm, a significant improvement over other platforms used by the same group for pioneering experiments on single molecule DNA detection and sequencing.<sup>19,38</sup> One important aspect to be mentioned regarding the use of  $\text{Si}_3\text{N}_4$  membranes in the plasmonic solid-state nanopore is that while they are demonstrated to be suitable for single molecule detection by means of an electrical readout, in the case of optical spectroscopies the  $\text{Si}_3\text{N}_4$  shows a background photoluminescence that limits the signal-to-noise ratio. In fact,  $\text{Si}_3\text{N}_4$  deposited by chemical vapor deposition contains silicon nanocrystals and defects which cause quantum confinement and a consequent photoluminescence. In order to solve this issue, alternative materials have been recently proposed such as  $\text{SiO}_2$ <sup>34</sup> and  $\text{TiO}_2$ .<sup>38</sup> They provide at least 1 order of magnitude background photoluminescence reduction over  $\text{Si}_3\text{N}_4$  and thus can be used for plasmonic nanopore applications.

Whereas a “plasmonic nanowell” enables enhanced optical detection, a simple circular cavity in a metallic layer is not the most efficient design to confine the e.m. field at the nanoscale. As mentioned for the case of ZMWs, the use of plasmonic nanoantennas facilitates the ability to engineer the e.m. field.<sup>39</sup> An important work (Figure 3b) that proposes a new concept of plasmonic nanostructures for nanopore sequencing is that reported by Belkin et al. in 2015.<sup>40</sup> Although only theoretical,

this manuscript investigated a solid-state nanopore coupled with plasmonic antennas and hypothesizes that a highly confined plasmonic field can ensure nanometer resolution to decode the DNA sequence during the translocation through a nanopore by means of optical spectroscopy (SERS). In particular, the authors proposed that bowtie antennas can enable spectroscopic fingerprints at a “few-nucleotide” resolution and that plasmonic trapping effects can control the translocation velocity.<sup>40</sup> In recent years, several types of plasmonic nanoantenna–nanopore configurations were reported, in particular by Dekker and co-workers.<sup>41–43</sup> These particular designs enable electro-optical measurements and at the same time behave as optical label-free detectors which monitor plasmonic resonance shift due to DNA translocation (Figure 3c). On the same line, giant fields created by plasmonic nanogaps can enable single-molecule SERS (Figure 3d).<sup>36</sup> In SERS, the vibrational modes of molecules very close ( $\sim 1$  nm) to the metal surface are detected, owing to the enhanced electromagnetic fields. This necessitates removing a proper recognition layer for specifying attachments as the molecules would be too far from the surface but does allow one to obtain molecular fingerprints from the spectrum. It is well-known that every molecule has its own Raman fingerprint and this is related to the building blocks of the biomolecules such as DNA, RNA, and proteins. The ability of SERS to produce these fingerprints with single molecule sensitivity can be of paramount importance for potential plasmonic sequencing applications. In attempts to reach high and reproducible SERS signals, several types of plasmonic pores have been tested in recent years<sup>44</sup> showing that the approach is potentially a winning strategy. Recently, Van Dorpe and co-workers studied DNA adsorbed inside a plasmonic nanoslit, reporting a spectroscopic library of nucleotides identified with single-molecule sensitivity.<sup>36</sup> They observed that the SERS signals are affected by the stochastic process of translocation through the nanoslit. This makes this spectroscopic method still challenging for sequential reads along a DNA strand. Although a plasmonic nanopore has the potential of manipulating nano-objects by plasmonic gradient forces, measuring DNA translocations in real-time with optical readout still requires significant improvement. Translocation of DNA through a plasmonic nanopore is still too fast for a spectrometer, and the differential affinities of nucleotides to the pore may also introduce uncertainties in detection. Recently, Huang et al. demonstrated single-nucleotide sensitivity in plasmonic nanopores coupled with molecular-coated plasmonic nanostars trapped inside the pore.<sup>45</sup> It is worth mentioning that this latter example did not use few nanometer scale nanopores, but a plasmonic trapping mechanism and the consequential single-molecule sensitivity is achieved in a so-called “nanocavity” generated in the narrow gap between a metallic nanostar and the wall of a 200 nm large plasmonic pore. These pioneering results demonstrate that a SERS–SMS system as envisioned by Belkin et al. a few years ago is worth being explored.

#### Additional Functionalities of Plasmonics Nanopores.

Currently, the ability of plasmonic nanostructures to control molecular translocation through the nanopore is a major challenge undertaken by several groups.<sup>33,46,47</sup> Solid-state structures may enable another modality of controlling the translocation kinetics so that SMS could be achieved. Toward this goal several techniques based on plasmonic driven effects (trapping, heating, etc.) have been proposed so far. One of the attractive effects is localized optical heating.<sup>39,48,49</sup> The

temperature gradient created by localized optical heating must take into account not only the increase of electrolyte conductivity but also thermal diffusion of ions (thermophoresis). This results in ion current enhancement and change in molecular capture rates that are a direct result of the thermal gradients that form near the pore.<sup>41</sup> In this context, the ionic current equation was proposed to estimate the temperature inside the nanopore and its dependence on solution conductivity and ion thermophoresis, (Figure 3e).<sup>50</sup>

$$\frac{I(T)}{I(T_{\text{room}})} = \frac{C}{C_0} \left[ \frac{X + Y(\Delta T + T_{\text{room}})}{X + YT_{\text{room}}} \right] \quad (1)$$

$$\frac{C}{C_0} = \exp[-S_T(T - T_{\text{room}})] \quad (2)$$

$$S_T = S_T^\infty \left[ 1 - \exp\left(\frac{T^* - T}{T_0}\right) \right] \quad (3)$$

where  $X$  and  $Y$  are electrolyte constants,  $C$  is the equilibrium ion concentration,  $C_0$  is the bulk species concentration,  $S_T$  is the Soret coefficient,  $T_{\text{room}}$  is the room temperature,  $S_T^\infty$  is a high- $T$  thermophoretic limit,  $T^*$  is the temperature where  $S_T$  switches sign, and  $T_0$  is the strength of temperature effects. These variables are available in Yamazaki et al. for pore temperature estimation<sup>50</sup> as well as Duhr et al. for theoretical thermophoresis explanation.<sup>51</sup> This rapid optical control of nanopore temperatures can be useful for studying single-molecule thermal kinetics with sub-microsecond time scale resolution, capturing a target molecule, and so on.<sup>50,52</sup>

The extreme light concentration by the plasmonic nanoantenna has been used to trap nanometer-sized molecules/particles inside nanoantennas or nanoslits,<sup>53</sup> and simulations have predicted that this optical force can be used for controlling the translocation of a polynucleotide molecule.<sup>40</sup> In principle, plasmonic nanoantennas equipped with a nanogap can achieve extremely localized e.m.-field intensity ( $|E|^2$ ) enhancements of up to  $10^4$  when the gap mode is excited. By controlling the size of the nanogaps, the confinement of the optical field can be tailored such that only a single molecule can fit the sensing volume. Moreover, the electromagnetic-field enhancement depends on the gap size and it dramatically increases with decreasing gap size.<sup>54</sup> The strongest field enhancements are created in gaps of  $\sim 1$  nm in size,<sup>55</sup> as nonlocal effects limit further enhancement for smaller gap sizes.

Apart from DNA sequencing, protein conformational dynamics including flexibility, binding kinetics, folding/unfolding, and so on are interesting research topics to explore with plasmonic nanopore systems. The extremely localized electromagnetic-field at a nanogap is useful for trapping individual protein molecules and, for example, monitoring protein conformational states.<sup>53</sup> Although nanopores can analyze unlabeled proteins,<sup>47,56</sup> the integration of plasmonic structures and nanopores can be the most promising approach to overcome the limited temporal resolution of nanopore measurements, as well as the low capture rates of molecules in the absence of a pore. This may allow the examination of molecules over longer times and with higher signal-to-noise values than standard fluorescence microscopy methods under a variety of conditions (low/high pH, low/high temperature, presence of ligands, and so forth; Figure 3f).<sup>57</sup>

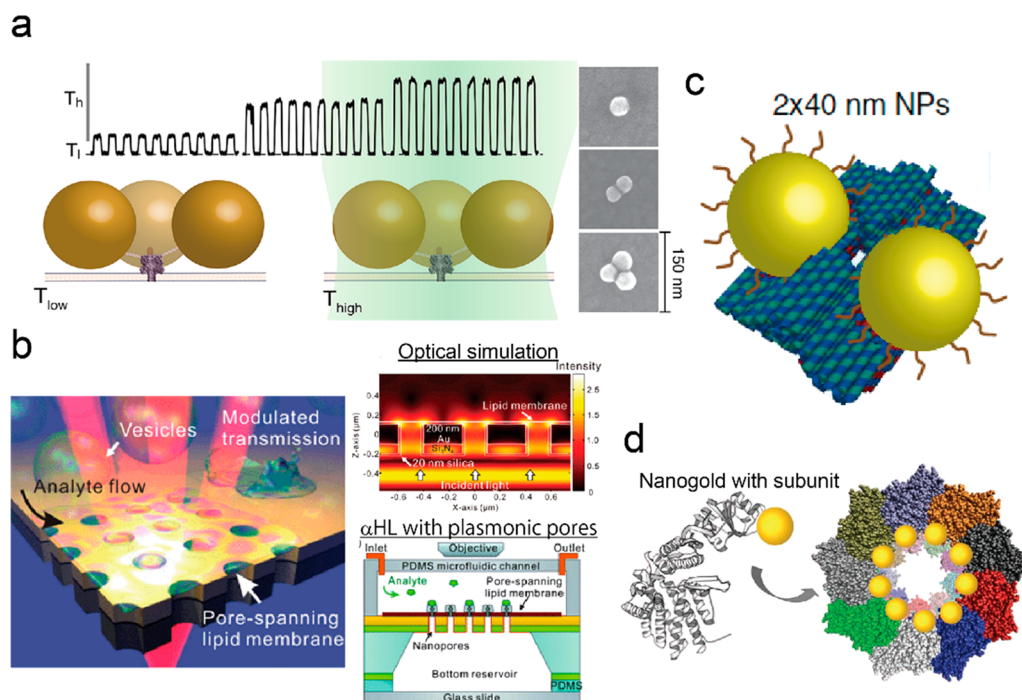


**Figure 4.** Plasmonic biological nanopore. (a) AuNP-tethered  $\alpha$ -hemolysin. The 30-basepair duplex DNA was used to tether gold nanoparticles (AuNPs) to  $\alpha$ -hemolysin. When visible light excites the AuNPs, the energy absorbed is transferred as local heating on the surrounding medium, resulting in the enhancement of current proportionally to temperature. Adapted with permission from ref 61, copyright 2013 American Chemical Society. (b) A free-standing Au nanoarray spanning lipid bilayer. Two hundred nanometer Au was deposited onto a free-standing SiN membrane, followed by 200 nm arrays using FIB. The platform provides enhanced e.m. fields at the edges. These e.m. fields report on  $\alpha$ -hemolysin incorporation, as well as antibody binding to  $\alpha$ -hemolysin. Adapted with permission from ref 62, copyright 2010 Royal Society of Chemistry. (c) AuNP dimers with DNA nanoplate containing a nanohole. Two AuNPs are facing with sub-5 nm spacing where a nanohole can be integrated. The dimension of DNA nanoplate is  $40 \times 45 \text{ nm}^2$ . SRES signals of dyes/nucleotides at strong e.m. field between AuNPs were observed. Adapted with permission from ref 63, copyright 2014 Springer Nature. (d) Self-assembled chaperonin subunit with AuNP. A 1.4 nm GNP is covalently attached to subunits of the pore beta chaperonin. A maximum of 18-GNPs can be integrated because 18 subunits assemble the chaperonin. Adapted with permission from ref 64, copyright 2002 Springer Nature.

Finally, it is worth noticing that plasmonics can also enable new nanopore fabrication methods. In particular, the excitation of a plasmonic nanoantenna on a dielectric membrane localizes the high-voltage-driven breakdown of the membrane to the hotspot of the enhanced optical field, creating a nanopore that is automatically self-aligned to the plasmonic hotspot.<sup>43</sup> Among the different methods for solid-state nanopore fabrication,<sup>58</sup> dielectric breakdown has been proposed as a powerful method that uses an external applied voltage to create a tiny hole in a dielectric membrane;<sup>12</sup> its application along with a plasmonic nanoantenna allows for an increase in efficiency of the phenomena driven by external light stimuli. To note, enhanced e.m. fields have also been used to create “self-aligned” nanopores in graphene membranes coupled with plasmonic nanoantennas.<sup>48</sup>

**Recent Advances on Integrated/Hybrid Designs.** The new functionalities offered by plasmonics in the field of solid-state nanopore are even more interesting if we consider new families of nanopores now under investigation. In particular two main classes of “advanced” nanopores can be found in the literature, that is, hybrid biological–solid-state pores and integrated nanopore designs comprising 2D materials.

Regarding hybrid structures, it has been recently demonstrated that a water-soluble viral portal nanopore assembly can be reproducibly integrated into a solid-state pore.<sup>59</sup> This is one of the very few examples of experimental demonstration of a biological nanopore integrated in a solid-state platform. In

particular, Hall et al.<sup>60</sup> showed how the handling and the alignment of a transmembrane protein ( $\alpha$ -hemolysin, etc.) to a prepatterned pore in a semiconductor membrane is at the same time extremely fascinating and challenging. Hybrid systems comprising plasmonic nanostructures have been also reported. In fact, not only do plasmonic nanopores significantly improve solid-state platforms but plasmonics can also facilitate biological nanopores. The challenge of plasmonic biological nanopores lies in engineering the plasmonic nanostructure nearby a pore supported by a lipid bilayer with nanometer precision. To the best of our knowledge, two main approaches have shown how to integrate the plasmonic nanostructure into a biological channel for sensing purpose: (i) the plasmonic nanoparticle links directly to biological pore (Figure 4a);<sup>61</sup> and (ii) the biological pore inserts into the supported lipid bilayer over plasmonic nanoholes (Figure 4b).<sup>62</sup> In the first platform, Reiner et al. introduced DNA to tether gold nanoparticles (AuNPs) to  $\alpha$ -hemolysin. Laser illumination causes local heating that increases ion current flow. Their observation of PEG translocation dynamics at different temperatures predicted unprecedented blockade shifts which might be due to the polymer’s physical/chemical properties or channel reorganization. The first platform can be extended to a variety of protein channels since self-assembly of functionalized nanoparticles using biological building blocks, such as DNA origami and chaperonin (Figure 4c,d) have been explored/studied for a decade.<sup>63,64</sup>

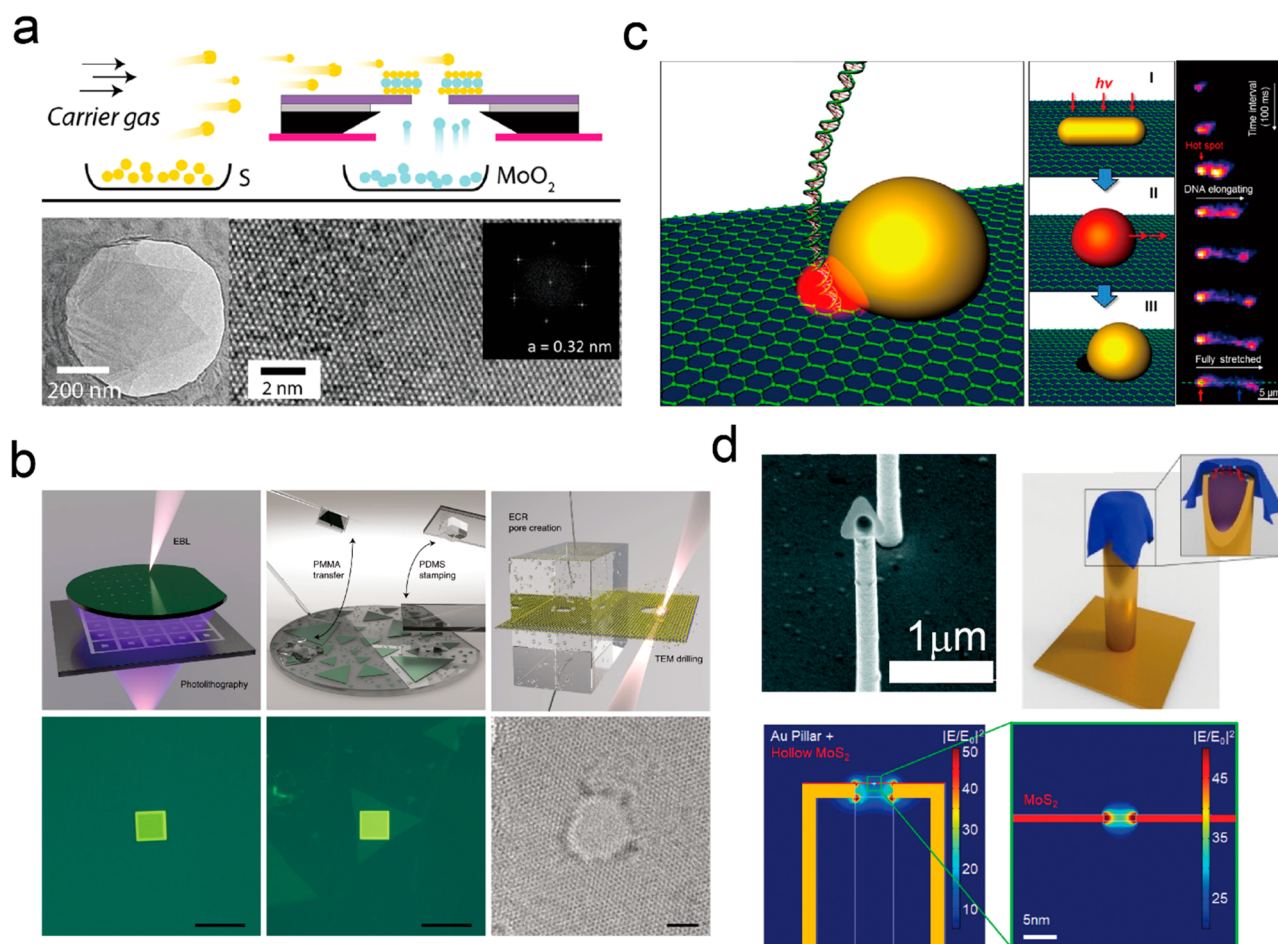


**Figure 5.** Approach toward 2D nanopore with plasmonic structure. (a) Chemical vapor deposition (CVD)-based fabrication of molybdenum disulfide ( $\text{MoS}_2$ ) membrane on solid-state aperture. Nanothick silicon nitride chip with micron-aperture is placed on top of molybdenum dioxide ( $\text{MoO}_2$ ). By flowing sulfur vapor at high temperature ( $\sim 750^\circ\text{C}$ ),  $\text{MoO}_2$  sublimates to generate nucleation site to grow  $\text{MoS}_2$ , leading to a few layers of polycrystalline  $\text{MoS}_2$  sealing on aperture. Adapted with permission from ref 69, copyright 2015 American Chemical Society. (b) Transferred  $\text{MoS}_2$  membrane with a nanopore. (Top) Schematic diagrams of solid-state aperture fabrication,  $\text{MoS}_2$  transfer, and nanopore drilling. (Bottom) An optical micrograph of solid-state aperture before and after  $\text{MoS}_2$  transfer, and TEM image of drilled nanopore. Adapted with permission from ref 70, copyright 2019, Springer Nature. (c) Graphene nanopore with plasmonic antenna. Preplaced-gold nanorods on graphene are photothermally heated to melting by femto-second laser illumination. Melted gold nanorod is reshaped into sphere and oxidizes the graphene surface to mill a pore, which is confirmed by optically monitoring dye-stained DNA translocation (right images). Adapted with permission from ref 48, copyright 2014 American Chemical Society. (d)  $\text{MoS}_2$  flakes on plasmonic nanostructures.  $\text{MoS}_2$  flakes arrive at the alkanedithiol-terminated gold hole by self-diffusion, which promotes their binding to the surface. Both the  $\text{MoS}_2$ -capped gold nanohole and the  $\text{MoS}_2$  nanopore show electromagnetic field enhancement of up to 2 orders of magnitude. Adapted with permission from ref 71, copyright The Royal Society of Chemistry 2018.

In the second main approach, first proposed by Im et al., it is possible to optically monitor the binding kinetics between antibodies and  $\alpha$ -hemolysin inserted into a lipid bilayer spanning over periodic plasmonic nanoholes. The strong local light intensity at the edge of the plasmonic holes interacts with  $\alpha$ -hemolysin, which leads to a red-shift of the plasmon resonance wavelength. A further shift was also observed when an antibody binds to  $\alpha$ -hemolysin. Although the second platform has not demonstrated simultaneous opto-electrical measurements, this can be an electro-optical device because many groups demonstrate ion/molecular detection using a protein channel in a supported lipid bilayer, as reported in a recent review from Demarche et al.<sup>65</sup>

Interesting results can also be obtained with a new class of integrated nanopores based on 2D materials.<sup>66</sup> An atomic thick membrane enables spatial resolution comparable with the interdistance between nucleic acids or amino-acids in

biopolymers. During the recent years several examples of single-molecule detection and sequencing by using 2D materials have been reported<sup>67</sup> but significant challenges must still be overcome, including compatibility with various electrolyte solutions, prevention of nonspecific adsorption, and the reproducibility of pore profiles and the resulting optoelectronic signals. In almost all cases, the electric read-out scheme was used to perform single nucleotide or single protein detection, with the consequent limitations reported above. It is worth mentioning the pioneer works from Radenovic's group that introduced the use of ionic liquids to control the translocation of DNA through the 2D-material pore to achieving SMS.<sup>68</sup>

In the field of 2D material, a 2D-plasmonic nanopore where the intrinsic in-plane e.m. field in atomic thin 2D materials is localized has been developed. This would represent a big step toward the next generation of remarkably improved nanopore



sensors thanks to the additional properties offered by plasmonics. Although a single layer of freestanding 2D membrane is achievable (Figure 5a,b),<sup>69,70</sup> the preparation of a nanopore in an atomically thick layer of 2D material remains a challenging task. It requires the deposition of single layers on top of a solid-state pore/membrane with a successive step involving a high-resolution electron beam sculpting/drilling process that often suffers from process variability, precluding the platform from being scalable.<sup>69</sup> Moreover, although large, continuous, and stable films of 2D materials can now be grown chemically to form free-standing membranes, their integration with plasmonic nanostructures is still extremely challenging. In fact, to prepare an integrated plasmonic/2D material pore, the integration of metallic nanostructures must be achieved in close proximity to the 2D material pore (Figure 5c,d).<sup>48,71</sup> Integrated 2D material-plasmonic nanopores can combine characteristic effects of a 2D material pore such as single nucleotide step translocation into 2D nanopores.<sup>72</sup> In this view, an interesting detection scheme can comprise an atomic thick membrane to control the translocation and a metallic nanostructure to enhance photon emission from biomolecules after proper excitation.<sup>44</sup>

**Future Outlook.** Single-molecule sensing by plasmonic nanopores has been greatly evolving over the past decade. Nevertheless, the application of plasmonic nanopores for sensing purposes is currently an active research field in nanoscience as it represents a new approach to realize high-bandwidth and high-throughput detection from multiple nanopores simultaneously. Plasmonic nanopores make it possible to efficiently flow liquid through the pore and force molecules to the active detection sites (hotspot). Moreover, the possibility to integrate high-sensitivity optical sensing with electrical detection is useful in a number of ways. For instance, multicolor “bar-coding” of individual molecules can be used to tag specific DNAs and potentially allow precise quantifications of DNA/RNA transcripts/proteins at single-molecule levels. Additionally, integration of plasmonic pores with other optical methods that allow improvements in temporal bandwidth (e.g., fluorescence correlation spectroscopy) and methods that have high spatial sensitivity (e.g., FRET), could be used to further enhance the amount of information that comes from a single-molecule experiment.

Finally, what would the next avenue be for plasmonic nanopores? We outline a few possible directions for future studies: (1) the use of other media for the plasmonic device, for example, 2D materials, could result in high-resolution and high-speed sensing; (2) the use of plasmonic nanopores as filtration devices, given the right surface functionalization, for example, a polymer brush, which modulates the selectivity of the pores to various analytes; (3) combination of plasmonic cavities with biological pores can harness the advantages of both of these sensor types, affording high-reproducibility transport kinetics and high-sensitivity optical sensing; (4) plasmonic heating can be used to denature and linearize a protein molecule for feeding into nanopores that allows one to obtain protein sequence information. These and more encompass a surely interesting outlook to the future of plasmonic nanopore sensors.

## ■ AUTHOR INFORMATION

### Corresponding Authors

\*E-mail: [denis.garoli@iit.it](mailto:denis.garoli@iit.it).

\*E-mail: [wannunu@neu.edu](mailto:wannunu@neu.edu).

### ORCID

Denis Garoli: 0000-0002-5418-7494

Nicolò Maccaferri: 0000-0002-0143-1510

Meni Wanunu: 0000-0002-9837-0004

### Notes

The authors declare no competing financial interest.

## ■ REFERENCES

- (1) Halas, N. J.; Lal, S.; Chang, W.-S.; Link, S.; Nordlander, P. *Chem. Rev.* **2011**, *111* (6), 3913–3961.
- (2) Zeng, S.; Baillargeat, D.; Ho, H.-P.; Yong, K.-T. *Chem. Soc. Rev.* **2014**, *43* (10), 3426–3452.
- (3) Dahlin, A. B. *Analyst* **2015**, *140* (14), 4748–4759.
- (4) Spitzberg, J. D.; Zrehen, A.; van Kooten, X. F.; Meller, A. *Adv. Mater.* **2019**, *31* (23), 1900422.
- (5) Fyta, M. J. *Phys.: Condens. Matter* **2015**, *27* (27), 273101.
- (6) Eid, J.; Fehr, A.; Gray, J.; Luong, K.; Lyle, J.; Otto, G.; Peluso, P.; Rank, D.; Baybayan, P.; Bettman, B.; Bibillo, A.; Bjornson, K.; Chaudhuri, B.; Christians, F.; Cicero, R.; Clark, S.; Dalal, R.; deWinter, A.; Dixon, J.; Foquet, M.; Gaertner, A.; Hardenbol, P.; Heiner, C.; Hester, K.; Holden, D.; Kearns, G.; Kong, X.; Kuse, R.; Lacroix, Y.; Lin, S.; Lundquist, P.; Ma, C.; Marks, P.; Maxham, M.; Murphy, D.; Park, I.; Pham, T.; Phillips, M.; Roy, J.; Sebra, R.; Shen, G.; Sorenson, J.; Tomaney, A.; Travers, K.; Trulson, M.; Vieceli, J.; Wegener, J.; Wu, D.; Yang, A.; Zaccarin, D.; Zhao, P.; Zhong, F.; Korlach, J.; Turner, S. *Science* **2009**, *323* (5910), 133–138.
- (7) Shema, E.; Jones, D.; Shores, N.; Donohue, L.; Ram, O.; Bernstein, B. E. *Science* **2016**, *352* (6286), 717–721.
- (8) Olasagasti, F.; Lieberman, K. R.; Benner, S.; Cherf, G. M.; Dahl, J. M.; Deamer, D. W.; Akeson, M. *Nat. Nanotechnol.* **2010**, *5*, 798.
- (9) Manrak, E. A.; Derrington, I. M.; Laszlo, A. H.; Langford, K. W.; Hopper, M. K.; Gillgren, N.; Pavlenok, M.; Niederweis, M.; Gundlach, J. H. *Nat. Biotechnol.* **2012**, *30*, 349.
- (10) Kasianowicz, J. J.; Brandin, E.; Branton, D.; Deamer, D. W. *Proc. Natl. Acad. Sci. U. S. A.* **1996**, *93* (24), 13770–13773.
- (11) Goyal, P.; Krasteva, P. V.; Van Gerven, N.; Gubellini, F.; Van den Broeck, I.; Troupiotis-Tsailaki, A.; Jonckheere, W.; Péhau-Arnaudet, G.; Pinkner, J. S.; Chapman, M. R.; Hultgren, S. J.; Howorka, S.; Fronzes, R.; Remaut, H. *Nature* **2014**, *516*, 250.
- (12) Kwok, H.; Briggs, K.; Tabard-Cossa, V. *PLoS One* **2014**, *9* (3), No. e92880.
- (13) Gilboa, T.; Zrehen, A.; Girsault, A.; Meller, A. *Sci. Rep.* **2018**, *8* (1), 9765.
- (14) Yamazaki, H.; Hu, R.; Zhao, Q.; Wannunu, M. *ACS Nano* **2018**, *12* (12), 12472–12481.
- (15) Feng, J.; Liu, K.; Graf, M.; Lihter, M.; Bulushev, R. D.; Dumcenco, D.; Alexander, D. T. L.; Krasnozhan, D.; Vuletic, T.; Kis, A.; Radenovic, A. *Nano Lett.* **2015**, *15* (5), 3431–3438.
- (16) Soni, G. V.; Singer, A.; Yu, Z.; Sun, Y.; McNally, B.; Meller, A. *Rev. Sci. Instrum.* **2010**, *81* (1), 014301.
- (17) Sawaf, F.; Clancy, B.; Carlsen, A. T.; Huber, M.; Hall, A. R. *Nanoscale* **2014**, *6* (12), 6991–6996.
- (18) Cai, S.; Sze, J. Y. Y.; Ivanov, A. P.; Edel, J. B. *Nat. Commun.* **2019**, *10* (1), 1797.
- (19) Gilboa, T.; Torfstein, C.; Juhasz, M.; Grunwald, A.; Ebenstein, Y.; Weinhold, E.; Meller, A. *ACS Nano* **2016**, *10* (9), 8861–8870.
- (20) Kotsifaki, D. G.; Chormaic, S. N. Plasmonic optical tweezers based on nanostructures: fundamentals, advances and prospects. *Nanophotonics* **2019**, *8*, 1227.
- (21) Levene, M. J.; Korlach, J.; Turner, S. W.; Foquet, M.; Craighead, H. G.; Webb, W. W. *Science* **2003**, *299* (5607), 682–686.
- (22) Bauch, M.; Toma, K.; Zhang, Q.; Dostalek, J. *Plasmonics* **2014**, *9*, 781–799.
- (23) Ponzellini, P.; Zambrana-Puyalto, X.; Maccaferri, N.; Lanzanò, L.; De Angelis, F.; Garoli, D. *Nanoscale* **2018**, *10* (36), 17362–17369.
- (24) Puchkova, A.; Vietz, C.; Pibiri, E.; Wünsch, B.; Sanz Paz, M.; Acuna, G. P.; Tinnefeld, P. *Nano Lett.* **2015**, *15* (12), 8354–8359.

- (25) Khatua, S.; Paulo, P. M. R.; Yuan, H.; Gupta, A.; Zijlstra, P.; Orrit, M. *ACS Nano* **2014**, *8* (5), 4440–4449.
- (26) Flauraud, V.; Regmi, R.; Winkler, P. M.; Alexander, D. T. L.; Rigneault, H.; van Hulst, N. F.; García-Parajo, M. F.; Wenger, J.; Brugger, J. *Nano Lett.* **2017**, *17* (3), 1703–1710.
- (27) van Ginkel, J.; Filius, M.; Szczepaniak, M.; Tulinski, P.; Meyer, A. S.; Joo, C. *Proc. Natl. Acad. Sci. U. S. A.* **2018**, *115* (13), 3338–3343.
- (28) Ghenuche, P.; Mivelle, M.; de Torres, J.; Moparthy, S. B.; Rigneault, H.; Van Hulst, N. F.; García-Parajo, M. F.; Wenger, J. *Nano Lett.* **2015**, *15* (9), 6193–6201.
- (29) de Torres, J.; Ghenuche, P.; Moparthy, S. B.; Grigoriev, V.; Wenger, J. *ChemPhysChem* **2015**, *16* (4), 782–788.
- (30) Punj, D.; Ghenuche, P.; Moparthy, S. B.; de Torres, J.; Grigoriev, V.; Rigneault, H.; Wenger, J. *Wiley Interdisciplinary Reviews: Nanomedicine and Nanobiotechnology* **2014**, *6* (3), 268–282.
- (31) Punj, D.; Mivelle, M.; Moparthy, S. B.; van Zanten, T. S.; Rigneault, H.; van Hulst, N. F.; García-Parajo, M. F.; Wenger, J. *Nat. Nanotechnol.* **2013**, *8*, 512.
- (32) Baibakov, M.; Patra, S.; Claude, J.-B.; Moreau, A.; Lumeau, J.; Wenger, J. *ACS Nano* **2019**, *13* (7), 8469–8480.
- (33) Larkin, J.; Foquet, M.; Turner, S. W.; Korlach, J.; Wanunu, M. *Nano Lett.* **2014**, *14* (10), 6023–6029.
- (34) Larkin, J.; Henley, R. Y.; Jadhav, V.; Korlach, J.; Wanunu, M. *Nat. Nanotechnol.* **2017**, *12*, 1169.
- (35) Jadhav, V.; Hoogerheide, D. P.; Korlach, J.; Wanunu, M. *Nano Lett.* **2019**, *19* (2), 921–929.
- (36) Chen, C.; Li, Y.; Kerman, S.; Neutens, P.; Willems, K.; Cornelissen, S.; Lagae, L.; Stakenborg, T.; Van Dorpe, P. *Nat. Commun.* **2018**, *9* (1), 1733.
- (37) Assad, O. N.; Gilboa, T.; Spitzberg, J.; Juhasz, M.; Weinhold, E.; Meller, A. *Adv. Mater.* **2017**, *29* (9), 1605442.
- (38) Wang, R.; Gilboa, T.; Song, J.; Huttner, D.; Grinstaff, M. W.; Meller, A. *ACS Nano* **2018**, *12* (11), 11648–11656.
- (39) Jonsson, M. P.; Dekker, C. *Nano Lett.* **2013**, *13* (3), 1029–1033.
- (40) Belkin, M.; Chao, S.-H.; Jonsson, M. P.; Dekker, C.; Aksimentiev, A. *ACS Nano* **2015**, *9* (11), 10598–10611.
- (41) Nicoli, F.; Verschuere, D.; Klein, M.; Dekker, C.; Jonsson, M. P. *Nano Lett.* **2014**, *14* (12), 6917–6925.
- (42) Verschuere, D. V.; Pud, S.; Shi, X.; De Angelis, L.; Kuipers, L.; Dekker, C. *ACS Nano* **2019**, *13* (1), 61–70.
- (43) Pud, S.; Verschuere, D.; Vukovic, N.; Plesa, C.; Jonsson, M. P.; Dekker, C. *Nano Lett.* **2015**, *15* (10), 7112–7117.
- (44) Chen, X.; Ciraci, C.; Smith, D. R.; Oh, S.-H. *Nano Lett.* **2015**, *15* (1), 107–113.
- (45) Huang, J.-A.; Mousavi, M. Z.; Zhao, Y.; Hubarevich, A.; Omeis, F.; Giovannini, G.; Schütte, M.; Garoli, D.; De Angelis, F., Single-molecule DNA Bases Discrimination in Oligonucleotides by Controllable Trapping in Plasmonic Nanoholes. arXiv e-prints, **2019**.
- (46) Di Fiori, N.; Squires, A.; Bar, D.; Gilboa, T.; Moustakas, T. D.; Meller, A. *Nat. Nanotechnol.* **2013**, *8*, 946.
- (47) Yusko, E. C.; Johnson, J. M.; Majd, S.; Prangio, P.; Rollings, R. C.; Li, J.; Yang, J.; Mayer, M. *Nat. Nanotechnol.* **2011**, *6*, 253.
- (48) Nam, S.; Choi, L.; Fu, C.-c.; Kim, K.; Hong, S.; Choi, Y.; Zettl, A.; Lee, L. P. *Nano Lett.* **2014**, *14* (10), 5584–5589.
- (49) Crick, C. R.; Albella, P.; Kim, H.-J.; Ivanov, A. P.; Kim, K.-B.; Maier, S. A.; Edel, J. B. *ACS Photonics* **2017**, *4* (11), 2835–2842.
- (50) Yamazaki, H.; Hu, R.; Henley, R. Y.; Halman, J.; Afonin, K. A.; Yu, D.; Zhao, Q.; Wanunu, M. *Nano Lett.* **2017**, *17* (11), 7067–7074.
- (51) Duhr, S.; Braun, D. *Phys. Rev. Lett.* **2006**, *96* (16), 168301.
- (52) Zhang, M.; Ngampeerapong, C.; Redin, D.; Ahmadian, A.; Sychugov, I.; Linnros, J. *ACS Nano* **2018**, *12* (5), 4574–4582.
- (53) Pang, Y.; Gordon, R. *Nano Lett.* **2012**, *12* (1), 402–406.
- (54) Jain, P. K.; Huang, W.; El-Sayed, M. A. *Nano Lett.* **2007**, *7* (7), 2080–2088.
- (55) Zhu, W.; Esteban, R.; Borisov, A. G.; Baumberg, J. J.; Nordlander, P.; Lezec, H. J.; Aizpurua, J.; Crozier, K. B. *Nat. Commun.* **2016**, *7*, 11495.
- (56) Waduge, P.; Hu, R.; Bandarkar, P.; Yamazaki, H.; Cressiot, B.; Zhao, Q.; Whitford, P. C.; Wanunu, M. *ACS Nano* **2017**, *11* (6), 5706–5716.
- (57) Verschuere, D.; Shi, X.; Dekker, C. *Small Methods* **2019**, *3* (5), 1800465.
- (58) Zhang, Y.; Kong, X.-Y.; Gao, L.; Tian, Y.; Wen, L.; Jiang, L. *Materials* **2015**, *8* (9), 6277–6308.
- (59) Cressiot, B.; Greive, S. J.; Mojtabavi, M.; Antson, A. A.; Wanunu, M. *Nat. Commun.* **2018**, *9* (1), 4652.
- (60) Hall, A. R.; Scott, A.; Rotem, D.; Mehta, K. K.; Bayley, H.; Dekker, C. *Nat. Nanotechnol.* **2010**, *5*, 874.
- (61) Reiner, J. E.; Robertson, J. W. F.; Burden, D. L.; Burden, L. K.; Balijepalli, A.; Kasianowicz, J. J. *J. Am. Chem. Soc.* **2013**, *135* (8), 3087–3094.
- (62) Im, H.; Wittenberg, N. J.; Lesuffleur, A.; Lindquist, N. C.; Oh, S.-H. *Chemical Science* **2010**, *1* (6), 688–696.
- (63) Thacker, V. V.; Herrmann, L. O.; Sigle, D. O.; Zhang, T.; Liedl, T.; Baumberg, J. J.; Keyser, U. F. *Nat. Commun.* **2014**, *5*, 3448.
- (64) McMillan, R. A.; Paavola, C. D.; Howard, J.; Chan, S. L.; Zaluzec, N. J.; Trent, J. D. *Nat. Mater.* **2002**, *1* (4), 247–252.
- (65) Demarche, S.; Sugihara, K.; Zambelli, T.; Tiefenauer, L.; Vörös, J. *Analyst* **2011**, *136* (6), 1077–1089.
- (66) Liang, L.; Shen, J.-W.; Zhang, Z.; Wang, Q. *Biosens. Bioelectron.* **2017**, *89*, 280–292.
- (67) Arjmandi-Tash, H.; Belyaeva, L. A.; Schneider, G. F. *Chem. Soc. Rev.* **2016**, *45* (3), 476–493.
- (68) Feng, J.; Liu, K.; Bulushev, R. D.; Khlybov, S.; Dumcenco, D.; Kis, A.; Radenovic, A. *Nat. Nanotechnol.* **2015**, *10*, 1070.
- (69) Waduge, P.; Bilgin, I.; Larkin, J.; Henley, R. Y.; Goodfellow, K.; Graham, A. C.; Bell, D. C.; Vamivakas, N.; Kar, S.; Wanunu, M. *ACS Nano* **2015**, *9* (7), 7352–7359.
- (70) Graf, M.; Lihter, M.; Thakur, M.; Georgiou, V.; Topolancik, J.; Ilic, B. R.; Liu, K.; Feng, J.; Astier, Y.; Radenovic, A. *Nat. Protoc.* **2019**, *14* (4), 1130–1168.
- (71) Garoli, D.; Mosconi, D.; Miele, E.; Maccaferri, N.; Ardin, M.; Giovannini, G.; Dipalo, M.; Agnoli, S.; De Angelis, F. *Nanoscale* **2018**, *10* (36), 17105–17111.
- (72) Wells, D. B.; Belkin, M.; Comer, J.; Aksimentiev, A. *Nano Lett.* **2012**, *12* (8), 4117–4123.